Effects of Gap Size and Excitation Frequency on the Vibrational Behavior and Wear Rate of Fuel Rods

Zupan Hu[a], M. D. Thouless[a,b,*] and Wei Lu[a, *]

[a]*Department of Mechanical Engineering*
[b]*Department of Materials Science & Engineering*
University of Michigan
Ann Arbor, MI 48109, USA

[*] Corresponding author. Tel.: +1 734 647 7858 (W. Lu); fax: +1 734 647 3170
E-mail addresses: weilu@umich.edu (W. Lu), thouless@umich.edu (M.D. Thouless)

Abstract

Grid-to-rod fretting (GTRF) wear is a major cause of fuel leaks. Understanding its mechanism is crucial for improving the reliability of nuclear reactors. In this paper we present a three-dimensional, finite-element based approach, which reveals how the wear rate depends on the size of the gap between the grid and the fuel rod, and on the frequency of the excitation force. We show that these two factors affect the dynamic vibration of the rod, which leads to three different regimes: harmonic, period-doubling and chaotic. The wear rate in the harmonic regime is significantly larger than that in the other two regimes, and reaches a maximum when the excitation frequency is close to the resonant frequency of the system, which is dependent on the gap size. We introduce the concept of a critical gap size that gives the maximum wear rate, and we identify the properties and values of this critical gap size. A wear map is developed as a result of a large number of parametric studies. This map shows quantitatively the wear rate as a function of the gap size and excitation frequency, and will be a valuable tool for the design and optimization of the fuel assembly to reduce the risk of fuel leaks caused by GTRF.

(August 21, 2016)

1. Introduction

A major cause of fuel failure in a pressurized water reactor (PWR) is grid-to-rod fretting (GTRF). This accounts for about 74% of all fuel leaks and is responsible for costly shutdowns (Kim, 2009). GTRF is a phenomenon in which the turbulent flow of the coolant exerts excitation forces on the fuel rods, causing the rods to vibrate against the grid that supports them. This leads to fretting wear of the rod surfaces, *i.e.*, the zircaloy cladding around the fuel (Axisa et al., 1988; Kim, 2010c). While it has been recognized that the problem is caused by the complex interaction between the rod, grid and coolant (Bortoleto *et al.*, 2013; Kim *et al.*, 2001; Kim *et al*., 2006; Kovács *et al*., 2009; Lee *et al.*, 2005; Rubiolo and Young, 2009; Sung *et al.*, 2001; Yan *et al.*, 2011), there is a lack of quantitative understanding of how the wear rate depends on the size of the gap between the grid and the rod (referred to later as the "gap size"), and on the frequency of the excitation force (referred to later as the "excitation frequency"). In this study we address these two important factors and their roles in the GTRF problem.

The gap between a fuel rod and the grid depends on many factors. The rod is designed to be held in place by a compressive load between the grid and the rod, using an initial interference between the two components. However, this pre-load can be relaxed by creep and deformation during assembly (Kim, 2010a, c), transportation (Kim, 2010c), and operation (Wang *et al.*, 2013). During operation, a gap can open because of creep-down of the cladding (Wang *et al.*, 2013), or close again because of fuel swelling or expansion from hydride formation. A gap can also be created as a result of the formation of a wear scar (Chung and Lee, 2011; Kim, 2010c; Zhang et al., 2012). Therefore,

understanding how the fretting wear is affected by the gap is of critical interest in the design of nuclear reactors.

The gap size plays an important role in determining the wear rate. Multiple possible scenarios may work together. A close fit between the rod and grid is often associated with a larger contact pressure and frictional force, which tend to increase the wear rate when sliding happens. However, a sufficiently tight fit can restrict sliding at the contact interface, and therefore reduce the wear rate. A loose connection between the rod and grid may lead to a high dynamic impact loads during oscillation; this would increase the wear rate (Kim, 2009, 2013; Kim and Suh, 2008, 2009; Li et al., 2009; Zhang et al., 2014). However, if the gap between the rod and the grid is too large, the oscillation may not have sufficient amplitude to cause contact to happen at all; this would reduce the wear rate. Of course, this is not a desirable condition since the spacer grid will not be able to provide adequate support for the fuel rod, and wear may shift to adjacent supports.

The wear rate is also sensitive to the excitation frequency. The excitation force associated with the turbulent flow has dominant frequencies that depend on the mechanical design and flow velocity (Chen et al., 1995; Delafontaine and Ricciardi, 2012; Kim, 2010c; Yan et al., 2011). Conceptually, the wear rate is expected to increase with the fretting frequency (Lee *et al.*, 2005) and the vibration amplitude of the rod, since a higher fretting frequency means more fretting cycles per unit time, while a larger amplitude is associated with a larger force. However, the situation is subtler than a simple dependence on two parameters, because the fretting frequency and the vibration amplitude of the rod are not independent. The excitation frequency affects both the fretting frequency and the amplitude in a non-monotonic way, complicating the effect of

excitation frequency on wear. We found that as the excitation frequency varies, the rod may experience harmonic, period-doubling and chaotic modes of vibration (Shaw and Holmes, 1983). The dependence of the fretting frequency and amplitude of the rod on the excitation frequency may change dramatically when the vibration mode of the rod evolves from one regime to another.

Experimental studies of different designs of spacer grids suggest that larger gaps result in greater wear (Kim, 2009; Kim and Suh, 2008, 2009). However, the conclusions were tied to the specific conditions that were tested, and to a limited range of gap sizes. Numerical studies of the GTRF problem, and of the related problem of wear of vibrating heat-exchanger tubes, give inconclusive results. Some suggest that the wear rate may decrease with gap size (Rubiolo, 2006; Rubiolo and Young, 2008), while others give completely opposite predictions (Hassan *et al.*, 2002; Rubiolo and Young, 2009). Experiments based on displacement-controlled impact suggest that the wear rate increases with the number of fretting cycles (Lee *et al.*, 2005). However, as shown by Shaw and Holmes (1983), the effect of excitation frequency on the fretting frequency and vibration amplitude of a dynamic system, such as a rod, cannot be captured by a simple displacement-controlled system. This issue forms a major aspect of the present paper.

Most existing numerical models for GTRF have been based on 1-D simulations. While these models are capable of estimating how normal loads and displacements are affected by the geometry and vibration, they cannot provide local wear information, since this requires details about the contacts and local stresses (Hassan et al., 2005). In this paper we use 3-D finite-element modeling to explore (i) the dynamic response of a fuel rod under the driving forces of various frequencies induced by the coolant, (ii) the effects

of the gap size and initial interference on the wear rate of the rod, and (iii) the effect of the excitation frequency on the wear rate. There are two key contributions of this study. The first is the calculation of the critical gap size that generates the greatest wear. The second is the calculation that shows how this critical gap depends on the excitation frequency and dynamic response of the rod.

2. Numerical Method

A model of a fuel rod is shown in Fig. 1. The two ends of the rod are pinned. The center of the rod is constrained by four pins that are connected to springs, and the springs are connected to a fixed spacer grid. The stiffness of these springs reflects the effective stiffness of more complicated support structures. Although many modes of vibration will be exhibited by a fuel rod in a PWR, we limit this study to only the first mode of vibration, in which the maximum displacement is at the center of the rod. A gap or interference (defined as a negative gap) is established between the rod and the supports. This is adjusted as part of the numerical studies. The fuel rod is composed of a zircaloy cladding and UO_2 fuel pellets. The mass of the two materials is combined together when considering the vibration of the rod. However, it is assumed that the UO_2 is not bonded to the zircaloy, and does not contribute to the stiffness of the rod. The vibration of the rod is assumed to occur along a plane inclined at 45° to the x- and y-axes, with symmetry dictating that the amplitudes of the displacements in the x- and y-directions are the same. This symmetric loading will result in the maximum frictional work rate for a given force amplitude, however, it should be noted that the motion of the rod can be in any direction in real applications (Rubiolo, 2006; Rubiolo and Young, 2008). The nomenclature for the

parameters and a list of the non-dimensional groups used in this analysis are given in Tables 1 and 2.

Figure 2 shows a 3-D finite-element model of the rod and supports. The mesh around the contact areas was refined to capture the contact information accurately. In particular, the mesh was refined sufficiently to reduce any associated numerical errors to less than the error bars that appear on any figures. The length and width of the contact plates are 1.7 and 0.7 times of the outer radius of the rod, respectively. The contact plates are made from zircaloy, and their dynamic responses are described by springs that have a characteristic stiffness of k_s. Our simulations showed that the effect from any material damping of the support grid is negligible. The dynamic response of the system is modeled using ABAQUS implicit dynamics. The contact between the plates and the fuel rod is formulated using a master-slave contact pair: the surface nodes on the slave surface move to avoid penetration by the master surface. We validated our model by test calculations using the same dimensions, boundary conditions and material properties as those in experiments (Shin *et al*., 1978) and in other numerical simulations (Sauvé and Teper, 1987): the vibration displacements and the impact forces that we obtained were consistent with those published results as shown in Fig. 3. The detailed dimensions and boundary conditions for these comparisons are given in Shin *et al.* (1978).

The excitation force was modeled as a harmonic load, so that the effect of various frequencies could be studied. We investigated a large spectrum of gap sizes and excitation frequencies. For each calculation, we ran a transient simulation until a steady-state response emerged, or until we could determine that the response was chaotic. The chaotic response is expected to appear in some regimes during oscillating impact (Moon

and Shaw, 1983; Shaw, 1985; Shaw and Holmes, 1983). When periodic rod vibrations could be identified, we used the steady-state vibration response to compute and evaluate the wear rate. Otherwise, the behavior was identified as being chaotic. From the perspective of understanding GTRF, it is important to appreciate that chaotic behavior can emerge even when the driving force is harmonic.

The wear rate associated with different parameters was estimated using Archard's Law (Johnson, 1984). In the local form of this law, the evolution of the wear depth, w, with time t at any point (x, y) on a surface is given by

$$w(x,y,t) = \mu\chi\int_0^t p(x,y,t)d\Delta, \tag{1}$$

where t is time, $p(x,y,t)$ is the local contact pressure, μ is the coefficient of friction, χ is the wear coefficient, and Δ is the local slip distance. Since the friction coefficient and the wear coefficient depend on wear mechanisms as well as material and operational conditions. (Kim et al., 2006; Kim, 2010b; Rubiolo and Young, 2009), our results are presented using normalized parameters. In this study we defined an average wear rate, or the increase in depth per unit time, to evaluate and compare the rate at which the wear depth increased under various conditions. If the rod vibration reached a periodic steady-state, we divided the accumulated wear depth over a steady-state cycle by the total time of the cycle, which gives the wear rate. Error bars are determined based on the wear rate of five cycles. Consideration of additional cycles for the periodic vibration did not change the result. If no periodicity was observed, the vibration was identified as being chaotic.

3. Results

3.1 Vibrational response

Several studies (Moon and Shaw, 1983; Shen et al., 2012; Wei et al., 2011) have shown that the vibrational response of an object is sensitive to the excitation frequency, and may exhibit several types of vibrational behaviors. For the GTRF problem considered here, we first needed to determine whether the system could reach a steady-state mode of vibration. We identified three types of vibrations. In Type 1, the fuel rod impacted the plate in each cycle, and the vibration displacement was the same for each cycle. In Type 2, the fuel rod impacted the plate during each cycle, but the displacement varied between sequential cycles. In Type 3, the fuel rod might not impact the plate during some cycles, and the vibration was chaotic.

Figure 4 shows examples of these three types of vibrational responses. The time in these figures is normalized by the first resonant frequency for the vibration of the free rod; this was obtained by calculating the vibration mode of a free rod, without any support plates. The displacement in these figures is normalized by the cladding thickness. The first two examples of behavior illustrated are Types 1 and 2; they are both periodic, but have different periods. The vibrational period of the first type is the same as that of the excitation force; the period of the second type is greater than that of the excitation force. These two types are referred to as the harmonic and period-doubling regimes, respectively. The third example shown in Fig. 4 is Type 3. It is not periodic, and there may, or may not be, impact in any given cycle; therefore, it is referred to as the chaotic regime. This chaotic response arises because of the nonlinearity of the system; a detailed discussion about its origin can be found in Moon and Shaw (1983) and in Thompson and

Ghaffari (1982). The wear rate during chaotic vibrations is relatively low since the rate of impact with the plate is small.

Figure 5 shows the impact force in the harmonic regime. The impact force is defined as the integration of the contact pressure $p(x,y,t)$ over the contact area. The impact force and the slip during contact both increase with gap size. Therefore the wear rate increases with gap size in this regime. However, it should be noted that this trend persists only in the harmonic regime, because the contact force and slip change in a non-monotonic way in the other two regimes.

3.2 The effects of gap size and excitation frequency on the wear rate

Harmonic regime: We calculated the wear rate using the method discussed in Section 2. The maximum local wear rate (referred to later simply as the "wear rate"), W, was obtained by surveying all contact points in the contact area. The dependence of the wear rate on the gap size is shown in Fig. 6. The wear rate increases with the gap size, until it peaks at a critical gap size, and then drops suddenly. The correlation between the wear rate and the gap size in the harmonic regime can be understood by referring to Fig. 5. As the gap size increases, both the impact force and the slip distance increase. Therefore, the frictional work rate becomes larger, and the wear rate per cycle increases. The number of impacts per unit of time in the harmonic regime is given by the excitation frequency, and is independent of gap size. As a result, the wear rate increases with the gap size.

Beyond the critical gap size, the vibration becomes chaotic. In the chaotic regime, the vibration is not periodic and the wear rates are somewhat dependent on the specific sampling intervals that are chosen for evaluation. However, they are all very small in

comparison to the wear rate in the harmonic and period-doubling regimes, as shown in Fig. 6. The reason for the small wear rate is that the chaotic vibration significantly reduces the chance of contact between the fuel rod and the plate, as shown in Fig. 4(c). In the chaotic regime the vibrational behavior is fairly complicated owing to the lack of periodicity. However, for practical applications we do not need to worry much about this regime, since the wear rate is small. A comparison between the plots in Fig. 6 shows that the critical size of gap at which chaotic behavior occurs decreases as the normalized excitation frequency, f/f_n, increases.

Period-doubling regime: Figure 7 shows the relationship between the wear rate and the gap size at a lower excitation frequency, where the period-doubling regime appears. Although the wear rate still increases with the gap size in the period-doubling regime, it fluctuates more significantly. A comparison between Fig. 7 and Fig. 6 shows that the wear rate is smaller for those conditions where a period-doubling regime exists. However, it should be noted that there is no sharp boundary between the harmonic, period-doubling and chaotic regimes.

3.3 A wear rate map of the gap size and the excitation frequency

We performed a series of calculations similar to those used to produce Figs. 5 and 6, covering a large spectrum of gap sizes and excitation frequencies. The results are presented as a wear map in Fig. 8, which shows the dependence of the wear rate on the gap size and excitation frequency. In the harmonic regime, there is a critical gap that is associated with the maximum wear rate for each excitation frequency. When the gap exceeds this critical value, the vibration becomes chaotic and the wear rate drops dramatically.

We found that the maximum wear rate in the landscape of gap size and excitation frequency correlates with the natural resonance of the system, which is defined as the frequency of the first mode of free vibration of a system consisting of the rod and support plates. To determine the resonant frequency of the system, we applied an initial displacement to the rod that was large enough to cause contact between the rod and the plate. We then released the rod, and observed the vibration for the displacement at the middle of the rod. When the gap size was relatively small, we found that the vibration was dominated by the first mode, and that the resonant frequency of the system was, therefore, straightforward to determine. The dependence of the resonant frequency of the system on the gap size in this regime is shown in Fig. 9, which also shows how the nonlinearities become more significant as the gap size increases.

The plot of Fig. 9 is superimposed on the map given in Fig. 8. It will be seen that the curve appears generally to overlap the peaks in the wear-rate contours. In other words, the peak wear rates correspond to the resonance conditions. Although the amplitude of the excitation force does affect the magnitude of the wear rate, it has little effect on the location of these peak wear rates, because the resonant frequency of the system is independent of the loading amplitude. The dependence of the wear rate on the gap size and the excitation frequency becomes more complicated with the appearance of period-doubling and chaotic behavior, but the wear rates in these regimes are much smaller.

For a given excitation frequency and amplitude, there will be no wear if the gap size is larger than the vibration amplitude of a free rod. We simulated the vibration of a free rod under different excitation frequencies. Using the maximum vibration amplitude,

we can identify the wear and no-wear regimes. These are shown in Fig. 10 (as well as being partially shown in Fig. 8). When the excitation frequency is close to the resonant frequency of the free rod, or f/f_n=1, we have the largest possible gap size that results in some wear. However, as shown in Fig. 8, the wear rate is relatively small in this condition.

We can also gain some insights about the excitation frequency from the perspective of wear growth. The gap size increases as a result of wear. When the excitation frequency is relatively low, say close to or a little above f/f_n=1, the wear scar grows slowly. However, wear will occur over an extended time, continuing even when the gap becomes relatively large. On the other hand, in the harmonic regime, with a relatively high excitation frequency, the wear rate is large. The wear scar will initially grow quickly, but then decrease rapidly as the gap size increases, and the vibration becomes chaotic.

4. Discussion

In GTRF problems, the vibration frequencies of the fuel rod observed in tests (Kim, 2010c; Rubiolo and Young, 2009) or simulations (Rubiolo, 2006; Rubiolo and Young, 2008) are significantly smaller than the dominant frequencies of the turbulent flow (Delafontaine and Ricciardi, 2012; Yan et al., 2011). Instead, the vibration is more likely to be a resonant response to certain frequencies close to the natural frequency of a continuously supported rod (Choi et al., 2004). Indeed, we found that a resonant frequency can be defined for a system with a small gap between the support and the fuel rod, which results in a maximum wear rate. In real applications, the stiffness of the fuel rod may change over time when pellets start to bond to the cladding. However, the

results of Fig. 8 are presented in a non-dimensional form. Therefore, if the resonant frequency of the rod or of the system at any given time is determined through a separate FEA simulation, the maximum wear rate can be easily predicted using this figure, even if the boundary conditions such as the gap size, the rod stiffness or the dominant load amplitude are changed.

In this study we simulated a unit two-span spacer-grid segment of the fuel rod, and investigated gap formation at the center. It was assumed that there is sufficient support to the fuel rod at the end points. This model can also represent the case of a two-span/one-support spacer grid along the entire length of the fuel rod, after scaling the length of the rod. In real applications, simultaneous gap formation at multiple supports can happen, which makes the problem more complicated. However, the results of the simple model provided important understanding of how the gap size and excitation frequency affect the vibration and wear rate. We expect that the method and the understanding, such as using the resonant frequency of the system to determine the excitation frequency that results in the maximum wear rate for a given gap size, can be extended to more complicated situations. For instance, one can use a 1-D model to identify the system resonant frequency (Kim, 2010b), and then map the displacement to a 3-D model to calculate wear.

5. Conclusions

In this paper we investigated the effects of gap size and excitation frequency on the vibration and wear rate of a fuel rod using a 3D dynamic model. It was observed that the wear rate is sensitive to the vibration response of the system. One of the important observations of this work is that chaotic behavior occurs in such a system, even if it is

assumed that the forcing function from the fluid is periodic. The wear rate in the harmonic regime is significantly larger than that in the period-doubling or chaotic regimes. Based on simulations of a large spectrum of gap sizes and excitation frequencies, we found that there is a critical gap size resulting in a maximum wear rate, and that this critical gap depends on the excitation frequency. The peak wear rate appears to occur at vibrations corresponding to the natural resonance of the system, which also depends on the gap size. By avoiding the high-wear-rate regimes through geometrical design of the fuel assembly, the risk of fuel leak due to GTRF wear can be significantly reduced. For this purpose, our present study focused on quantifying and evaluating the effect of gap size on the wear rate. Tracking the growth of wear scars (Hu et al., 2015a; Hu et al., 2015b, 2016) as well as incorporating mechanisms such as creep is currently in progress.

Acknowledgements

This research was supported by the Consortium for Advanced Simulation of Light Water Reactors (http://www.casl.gov), an Energy Innovation Hub (http://www.energy.gov/hubs) for Modeling and Simulation of Nuclear Reactors under U.S. Department of Energy Contract No. DE-AC05-00OR22725.

References

Axisa, F., Antunes, J., Villard, B., 1988. Overview of numerical methods for predicting flow-induced vibration. Journal of Pressure Vessel Technology 110, 6-14.

Bortoleto, E.M., Rovani, A.C., Seriacopi, V., Profito, F.J., Zachariadis, D.C., Machado, I.F., Sinatora, A., Souza, R.M., 2013. Experimental and numerical analysis of dry contact in the pin on disc test. Wear 301, 19-26.

Chen, S.S., Zhu, S., Cai, Y., 1995. Experiment of chaotic vibration of loosely supported tube rows in cross-flow. Journal of Pressure Vessel Technology 117, 204-212.

Choi, M.H., Kang, H.S., Yoon, K.H., Song, K.N., 2004. Vibration analysis of a dummy fuel rod continuously supported by spacer grids. Nuclear Engineering and Design 232, 185-196.

Chung, I., Lee, M., 2011. An experimental study on fretting wear behavior of cross-contacting Inconel 690 tubes. Nuclear Engineering and Design 241, 4103-4110.

Delafontaine, S., Ricciardi, G., 2012. Fluctuating pressure calculation induced by axial flow trough mixing grid. Nuclear Engineering and Design 242, 233-246.

Hassan, M.A., Weaver, D.S., Dokainish, M.A., 2002. A simulation of the turbulence response of heat exchanger tubes in lattice-bar supports. Journal of Fluids and Structures 16, 1145-1176.

Hassan, M.A., Weaver, D.S., Dokainish, M.A., 2005. A new tube/support impact model for heat exchanger tubes. Journal of Fluids and Structures 21, 561-577.

Hu, Z., Lu, W., Thouless, M.D., 2015a. Slip and wear at a corner with Coulomb friction and an interfacial strength. Wear 338–339, 242-251.

Hu, Z., Lu, W., Thouless, M.D., Barber, J.R., 2015b. Simulation of wear evolution using fictitious eigenstrains. Tribology International 82, Part A, 191-194.

Hu, Z., Lu, W., Thouless, M.D., Barber, J.R., 2016. Effect of plastic deformation on the evolution of wear and local stress fields in fretting. International Journal of Solids and Structures 82, 1-8.

Johnson, K., 1984. Contact mechanics. Cambridge University Press, Cambridge, UK.

Kim, H.-K., Kim, S.-J., Yoon, K.-H., Kang, H.-S., Song, K.-N., 2001. Fretting wear of laterally supported tube. Wear 250, 535-543.

Kim, H.-K., Lee, Y.-H., Heo, S.-P., 2006. Mechanical and experimental investigation on nuclear fuel fretting. Tribology International 39, 1305-1319.

Kim, K.-T., 2009. The study on grid-to-rod fretting wear models for PWR fuel. Nuclear Engineering and Design 239, 2820-2824.

Kim, K.-T., 2010a. The effect of fuel rod loading speed on spacer grid spring force. Nuclear Engineering and Design 240, 2884-2889.

Kim, K.-T., 2010b. The effect of fuel rod supporting conditions on fuel rod vibration characteristics and grid-to-rod fretting wear. Nuclear Engineering and Design 240, 1386-1391.

Kim, K.-T., 2010c. A study on the grid-to-rod fretting wear-induced fuel failure observed in the 16×16KOFA fuel. Nuclear Engineering and Design 240, 756-762.

Kim, K.-T., 2013. Applicability of out-of-pile fretting wear tests to in-reactor fretting wear-induced failure time prediction. Journal of Nuclear Materials 433, 364-371.

Kim, K.-T., Suh, J.-M., 2008. Development of an advanced PWR fuel for OPR1000s in Korea. Nuclear Engineering and Design 238, 2606-2613.

Kim, K.-T., Suh, J.-M., 2009. Impact of nuclear fuel assembly design on Grid-to-Rod Fretting Wear. Journal of Nuclear Science and Technology 46, 149-157.

Kovács, S., Stabel, J., Ren, M., Ladouceur, B., 2009. Comparative study on rod fretting behavior of different spacer spring geometries. Wear 266, 194-199.

Lee, Y.-H., Kim, H.-K., Jung, Y.-H., 2005. Effect of impact frequency on the wear behavior of spring-supported tubes in room and high temperature distilled water. Wear 259, 329-336.

Li, X.C., Gu, H., Gao, X.L., 2009. Molecular Dynamics Study on Mechanical Properties and Interfacial Morphology of an Aluminum Matrix Nanocomposite Reinforced by -Silicon Carbide Nanoparticles. Journal of Computational and Theoretical Nanoscience 6, 61-72.

Moon, F.C., Shaw, S.W., 1983. Chaotic vibrations of a beam with non-linear boundary conditions. International Journal of Non-Linear Mechanics 18, 465-477.

Rubiolo, P.R., 2006. Probabilistic prediction of fretting-wear damage of nuclear fuel rods. Nuclear Engineering and Design 236, 1628-1640.

Rubiolo, P.R., Young, M.Y., 2008. VITRAN: an advance statistic tool to evaluate fretting-wear damage. Journal of Power and Energy Systems 2, 57-66.

Rubiolo, P.R., Young, M.Y., 2009. On the factors affecting the fretting-wear risk of PWR fuel assemblies. Nuclear Engineering and Design 239, 68-79.

Sauvé, R.G., Teper, W.W., 1987. Impact simulation of process equipment tubes and support plates—A numerical algorithm. Journal of Pressure Vessel Technology 109, 70-79.

Shaw, S.W., 1985. Forced vibrations of a beam with one-sided amplitude constraint: Theory and experiment. Journal of Sound and Vibration 99, 199-212.

Shaw, S.W., Holmes, P.J., 1983. A periodically forced impact oscillator with large dissipation. Journal of Applied Mechanics 50, 849-857.

Shen, X., Liu, Y., Cao, L., Chen, X., 2012. Numerical simulation of sliding wear for self-lubricating spherical plain bearings. Journal of Materials Research and Technology 1, 8.

Shin, Y., Sass, D., Jendrzejczyk, J., 1978. Vibro-impact responses of a tube with tube--baffle interaction. Argonne National Lab., Ill.(USA).

Sung, J.H., Kim, T.H., Kim, S.S., 2001. Fretting damage of TiN coated zircaloy-4 tube. Wear 250, 658-664.

Thompson, J.M.T., Ghaffari, R., 1982. Chaos after period-doubling bifurcations in the resonance of an impact oscillator. Physics Letters A 91, 5-8.

Wang, H., Hu, Z., Lu, W., Thouless, M.D., 2013. A mechanism-based framework for the numerical analysis of creep in zircaloy-4. J Nucl Mater 433, 188-198.

Wei, C., Chan, J., Garmire, D., 2011. 3-axes MEMS Hall-effect sensor, Sensors Applications Symposium (SAS), 2011 IEEE, pp. 141-144.

Yan, J., Yuan, K., Tatli, E., Karoutas, Z., 2011. A new method to predict Grid-To-Rod Fretting in a PWR fuel assembly inlet region. Nuclear Engineering and Design 241, 2974-2982.

Zhang, J., Johnston, J., Chattopadhyay, A., 2014. Physics-based multiscale damage criterion for fatigue crack prediction in aluminium alloy. Fatigue & Fracture of Engineering Materials & Structures 37, 119-131.

Zhang, J., Liu, K., Luo, C., Chattopadhyay, A., 2012. Crack initiation and fatigue life prediction on aluminum lug joints using statistical volume element–based multiscale modeling. Journal of Intelligent Material Systems and Structures.

Tables

Table 1: Nomenclature

D_c	thickness of the Zircaloy cladding
E	Young's modulus of the Zircaloy cladding
f	excitation frequency
f_n	resonant frequency of a free rod
F_a	amplitude of the excitation force
g	gap size
k_s	stiffness of the spring
L	half-length of the rod
p	local contact pressure
R	outer radius of the rod
t	time
U	displacement of the rod
w	wear depth
W	maximum local wear rate in the contact area (increase in depth per unit time)
Δ	slip distance
μ	coefficient of friction
ν	Poisson's ratio of the Zircaloy cladding
ρ	density of the Zircaloy cladding
χ	wear coefficient

Table 2: Values of non-dimensional parameters held fixed in all the calculations

L / D_c	920
R / D_c	7.5
$\frac{F_a}{D_c k_s}$	1.2×10^{-4}
μ	0.25
χE	3×10^{4}
$\frac{k_s}{E D_c}$	2×10^{-3}
$\frac{\rho L^2 f_n^{\,2}}{E}$	6×10^{-6}
ν	0.342

Figures

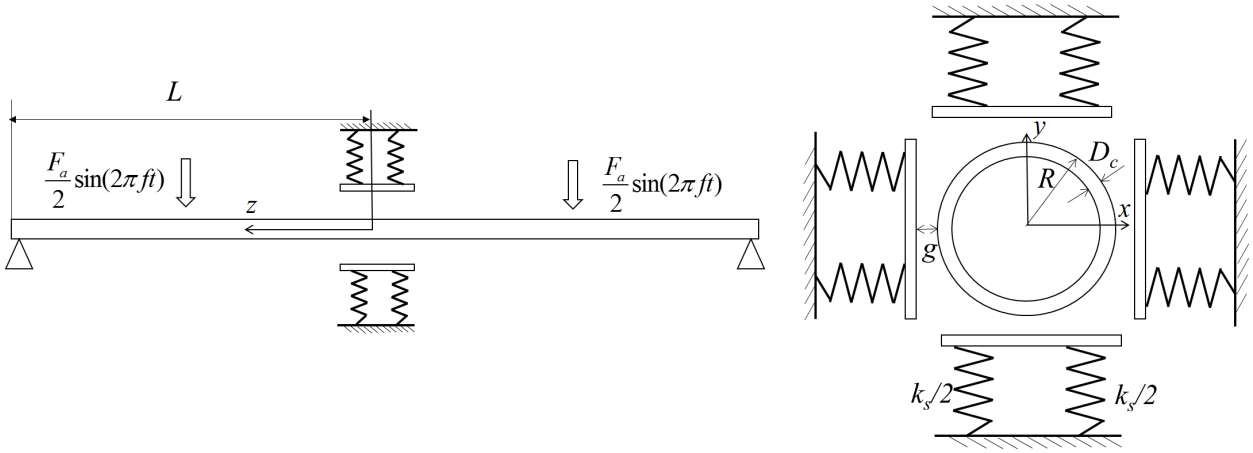

Figure 1. A schematic illustration of the model used for the GTRF simulation. The fuel rod has an outer radius of R with a cladding thickness of D_c. Four support plates are connected to springs with a stiffness of k_s. The gap between the fuel rod and the plate is g. The rod vibrates along a plane that is diagonal to the x- and y-axes.

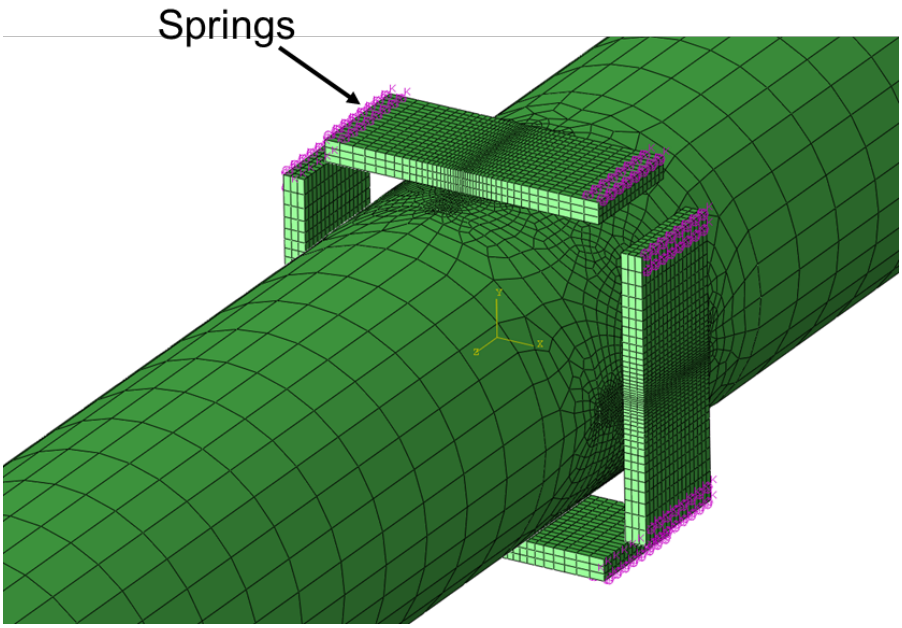

Figure 2. The 3-D finite-element model used for the dynamic simulations. Each plate is connected to ground springs with a total stiffness of k_s. Contact elements and refined meshes are used in the contact regions.

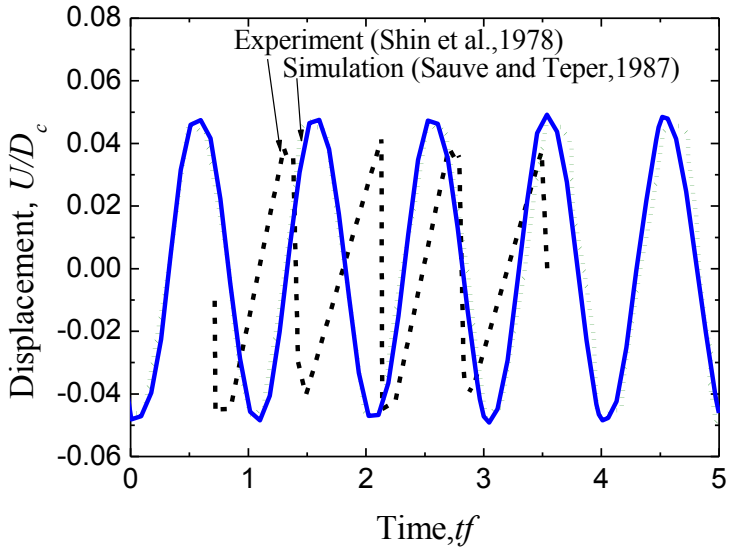

(a)

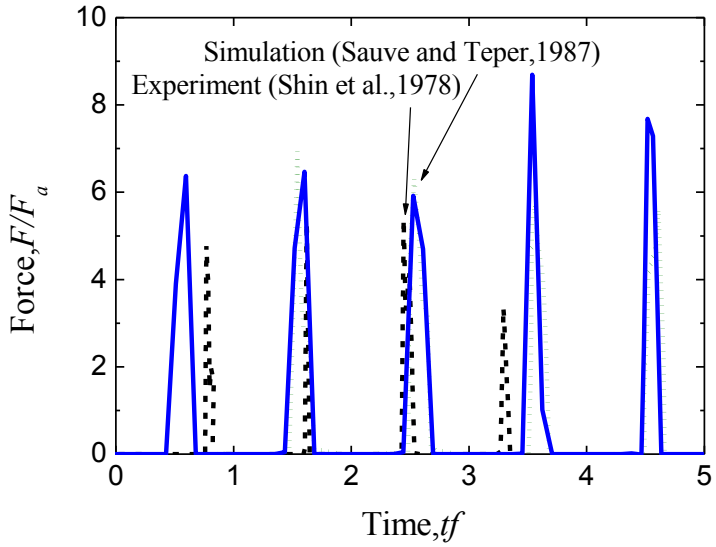

(b)

Figure 3. The displacement **(a)** and impact force **(b)** of the validation model are consistent with published experiments and numerical simulations.

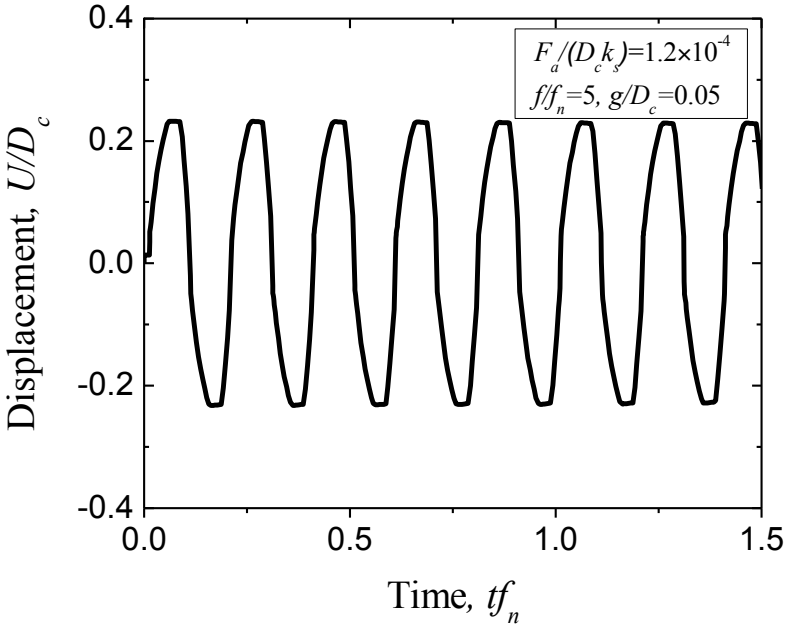
$F_a/(D_c k_s)$=1.2×10^{-4}
f/f_n=5, g/D_c=0.05
Displacement, U/D_c
Time, tf_n
0.4
0.2
0.0
-0.2
-0.4
0.0
0.5
1.0
1.5

(a)

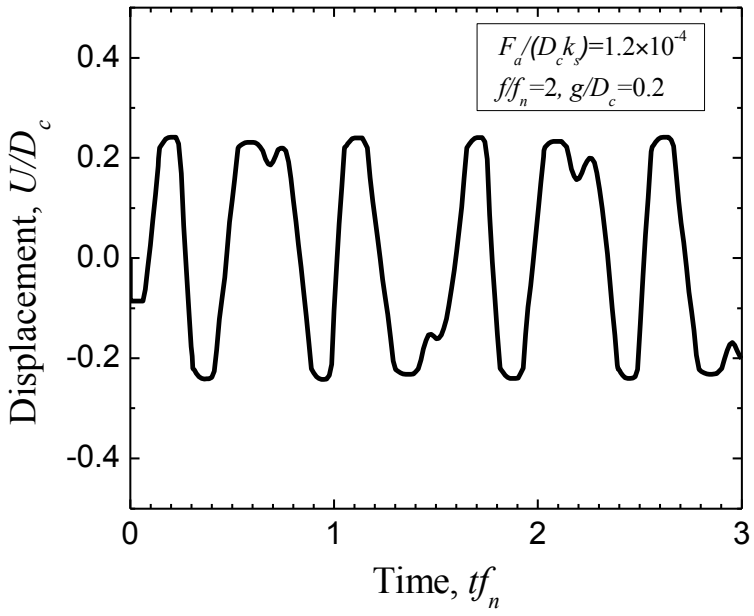
$F_a/(D_c k_s)$=1.2×10^{-4}
f/f_n=2, g/D_c=0.2
Displacement, U/D_c
Time, tf_n
0.4
0.2
0.0
-0.2
-0.4
0
1
2
3

(b)

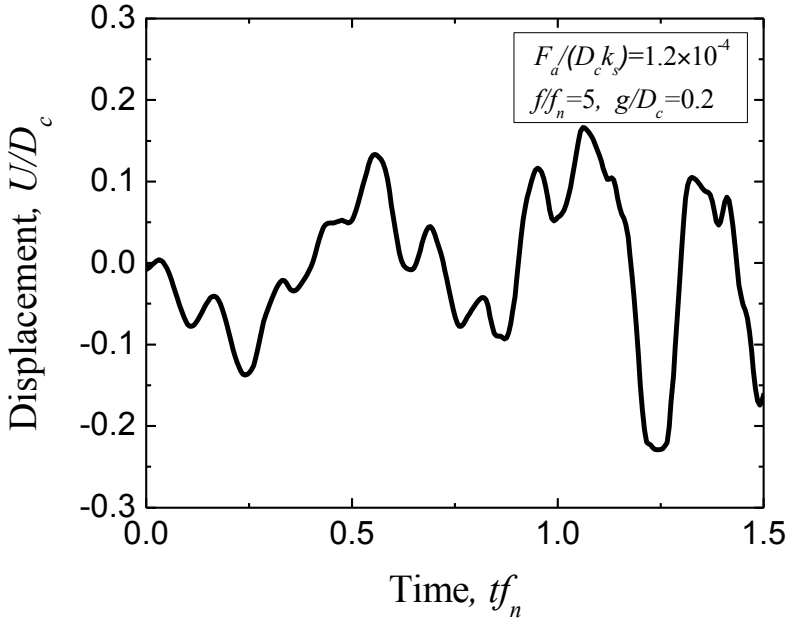

(c)

Figure 4. Three types of vibrations were observed in the simulations. **(a)** Type 1: the rod impacts the plate in each cycle. The vibration is periodic, and the period is equal to that of the excitation force. **(b)** Type 2: the rod impacts the plate in each cycle. The vibration is periodic but with a period greater than that of the excitation force. The period of the vibration changes with gap size. **(c)** Type 3: the rod may or may not impact the plate in any given excitation cycle, and the vibration is chaotic.

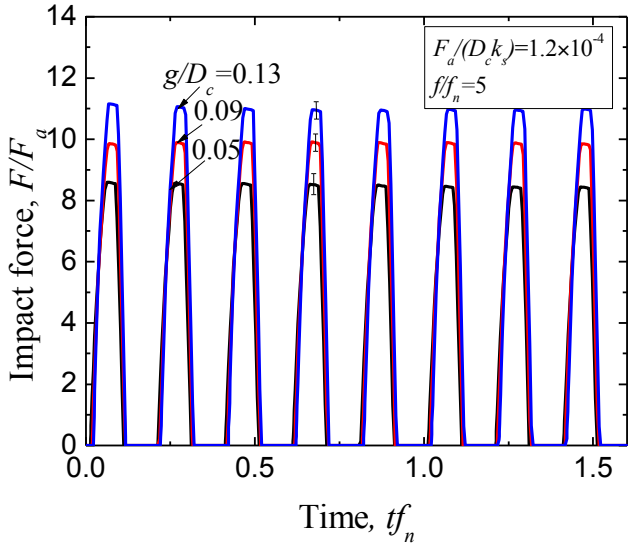

Figure 5. The impact force increases with the gap size, g/D_c, in the harmonic regime.

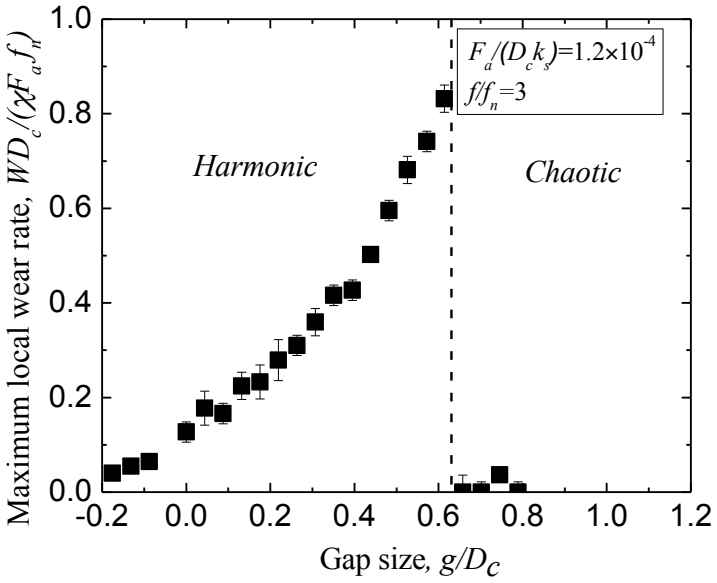
$F_a/(D_c k_s)$=1.2×10^{-4}
f/f_n=3
Harmonic
Chaotic
Maximum local wear rate, $WD_c/(\chi F_a f_n)$
Gap size, g/D_c

(a)

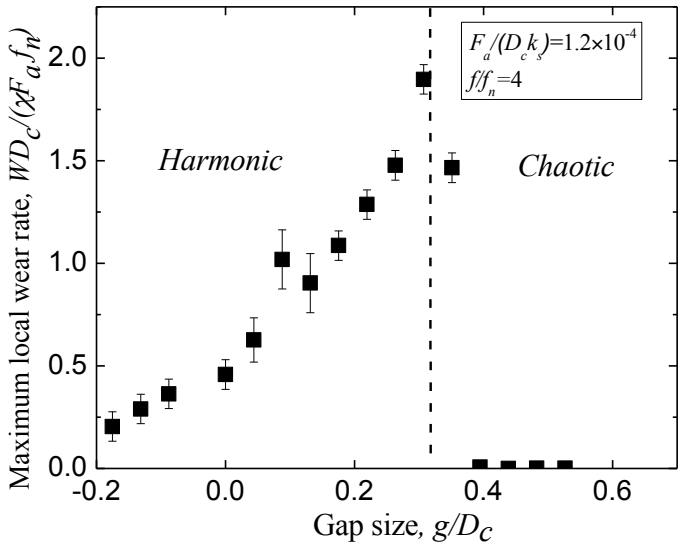
$F_a/(D_c k_s)$=1.2×10^{-4}
f/f_n=4
Harmonic
Chaotic
Maximum local wear rate, $WD_c/(\chi F_a f_n)$
Gap size, g/D_c

(b)

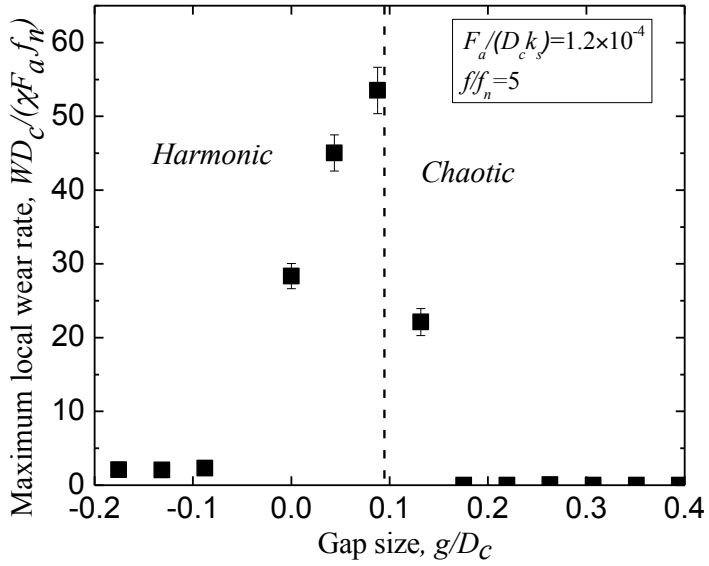

(c)

Figure 6. Plots of the relationship between the maximum local wear rate and the gap size at various excitation frequencies of f/f_n=3, 4 and 5. The wear rate with an interference (a negative gap size) is smaller than that with a gap. The wear rate increases with the gap size until it peaks at a particular gap that we call the critical gap size. Beyond this the vibration becomes chaotic and the wear rate drops dramatically.

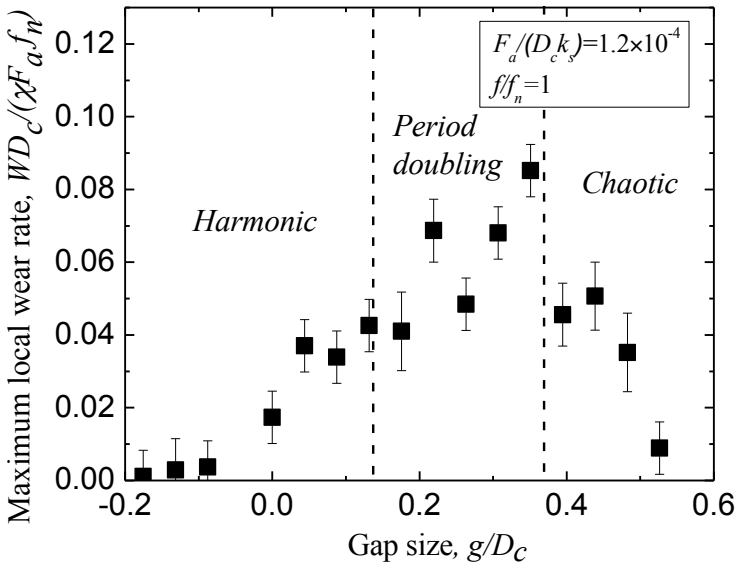

Figure 7. Plot of the relationship between the maximum local wear rate and the gap size at excitation frequencies of f/f_n=1. With the existence of a period-doubling regime, the wear rate is smaller than that in Fig. 5.

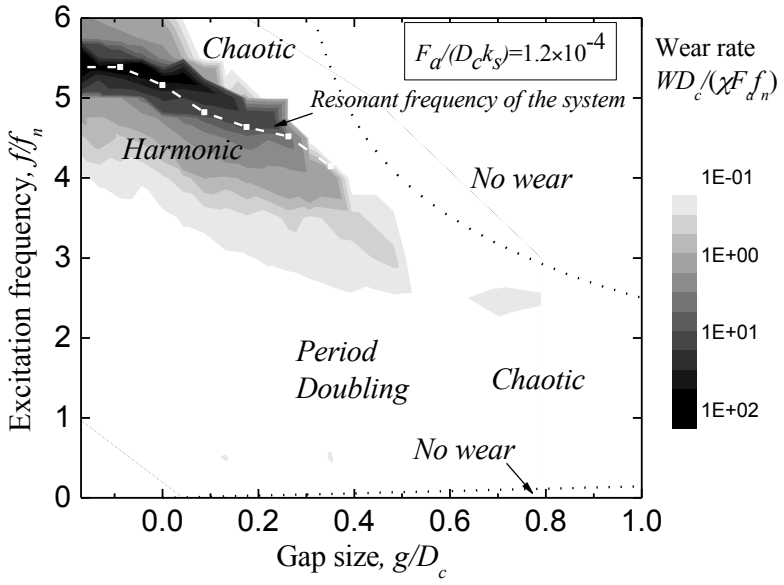

Figure 8. A wear-rate map for a large spectrum of gap sizes and excitation frequencies. The critical gap size, which is associated with the maximum wear rate, lies within the harmonic regime. In the no wear region the amplitude of the rod vibration is smaller than the gap size so that no impact between the rod and plate can happen. The curve of the resonant frequency of the system (from Fig. 8) appears to overlap with the peaks in the contour.

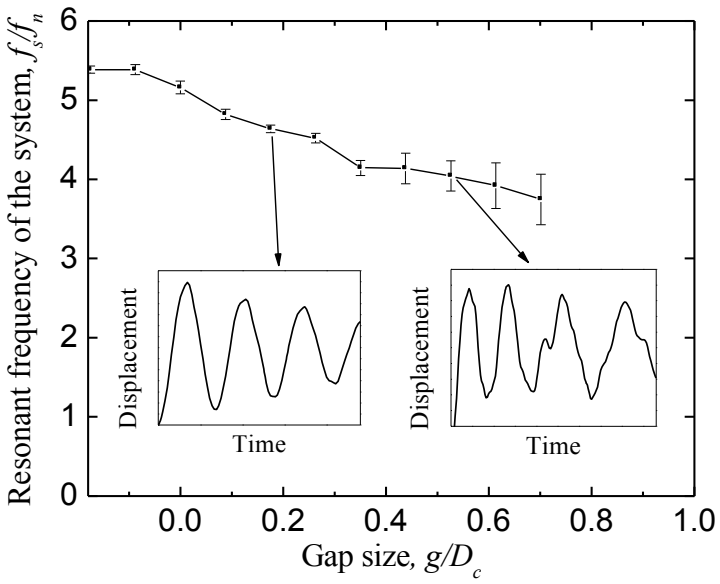

Figure 9. The dependence of the resonant frequency of the system, f_s, on the gap size. The behavior becomes more complicated when the gap size is large.

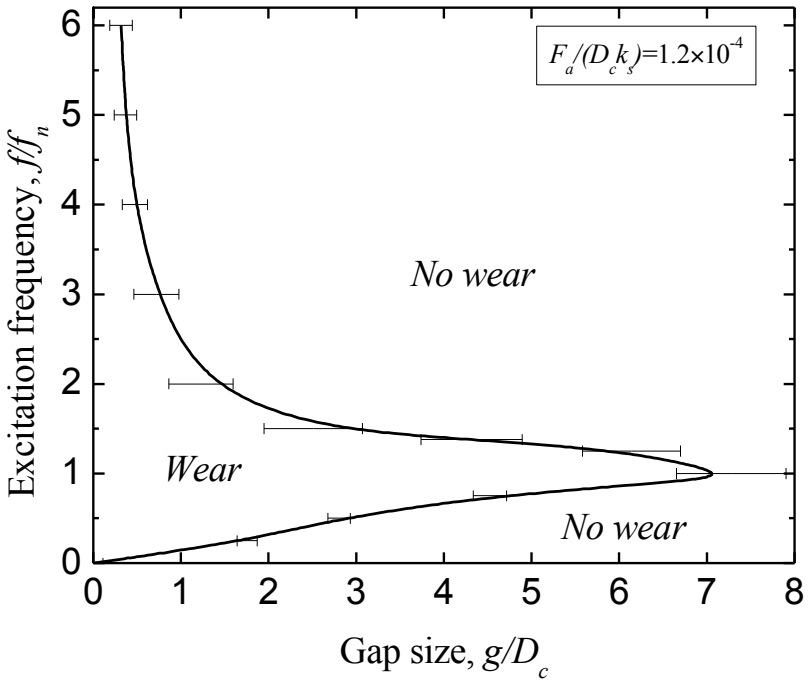

Figure 10. There is no wear if the gap size is larger than the vibration amplitude of the rod.